RSC Advances

PAPER

View Article Online
View Journal | View Issue



Cite this: *RSC Adv.*, 2026, **16**, 16105

# Synthesis of styrene polymer grafted nanocarbon particles for application as reinforcement additive for unsaturated polyester plastics

Bui Quynh Anh Nguyen, †[ac] Thi Phuong Loan Pham, †[ac] Thanh Huy Nguyen, [ac] Dieu Linh Dinh, [ac] Tri Hieu Pham, [ac] Huu Dat Nguyen,[ac] Thanh Tung Tran,[ac] Thi Quynh Anh Luong,[bc] Bui Anh Duy Nguyen *[ac] and Quoc Phu Phan *[ac]

The reinforcement of filler materials into an unsaturated polyester (UPE) matrix is often limited by agglomeration, leading to poor compatibility. Recently, nano-sized filler materials have attracted attention as effective reinforcement agents in UPE. In this study, styrene polymer-grafted carbon nanoparticles were synthesized using the solution plasma method and applied as reinforcing additives for UPE. The synthesis of nanoparticles was conducted directly in the styrene monomer environment, enabling the simultaneous formation of carbon nanoparticles and the grafting of polymer onto their surfaces *via* a free-radical mechanism. SEM analysis revealed more uniform particle dispersion and a polymer-coated surface in UPE/NC-gP samples, indicating increased compatibility with the matrix. FTIR also showed that the representative peaks C–H, C=C, C=O, and C–O oscillated clearly in the UPE/NC-gP samples. Notably, the use of styrene-grafted carbon nanoparticle significantly improved the tensile modulus, tensile strength, flexural modulus, and flexural strength of the UPE/NC-gP(1 h) sample to 479.89 ± 26.22, 39.23 ± 2.06, 1504.06 ± 55.18, and 44.67 ± 1.82 MPa, respectively, compared with UPE/SM. Meanwhile, the UPE/NC-gP(3 h) sample had the highest flexural stress and flexural modulus of 49.01 ± 3.03 and 1535.81 ± 58.47 MPa, respectively, but the flexural strain was low. The results indicate that the grafting time influences the properties of the UPE composite. This study confirms the potential of the solution plasma method for the fabrication of nanoadditives highly compatible with the polymer matrix, opening new avenues for the production of nanocomposite materials.

Received 19th November 2025
Accepted 13th March 2026

DOI: 10.1039/d5ra08954a

rsc.li/rsc-advances



## 1. Introduction

Unsaturated polyester resin (UPE) is one of the most widely used thermosetting polymers, with applications in construction, the automotive and marine sectors, and composite materials manufacturing (Fig. 1), owing to its high mechanical strength, corrosion resistance, and competitive production cost.[1–6] However, limitations in UPE's impact toughness and flexural strength restrict its use in high-performance applications.[7,8] Studies have explored the use of traditional fillers, such as stone powder, wood powder, flax, or $CaCO_3$, to enhance durability and reduce costs.[4,9–11] Nevertheless, these fillers are typically coarse, exhibit limited dispersion in the polymer matrix, and struggle to form a stable chemical bond with the UPE matrix.[4] Therefore, they often serve only as bulking agents rather than as effective reinforcing agents for the polymer matrix.[4] The uneven dispersion also creates stress concentrations, significantly reducing the material's overall strength.[9–11] Meanwhile, advanced reinforcing materials such as carbon fibers and glass fibers provide superior performance. Still, they are limited by high production costs, complex processes, high energy consumption, and the risk of toxic dust emissions, which affect worker health and the environment and make them difficult to align with the materials industry's sustainable development orientation.[5,6]

In this context, carbon nanoparticles are considered a breakthrough approach to enhancing polymer performance, owing to their unique morphological properties, including a large specific surface area, superior mechanical strength, and high electrical conductivity.[12–17] These properties significantly improve the mechanical, thermal, and electrical properties of

[a]*Department of Polymer Materials, Faculty of Materials Technology, Ho Chi Minh City University of Technology (HCMUT), 268 Ly Thuong Kiet Street, Dien Hong Ward, Ho Chi Minh City, Vietnam. E-mail: anh.nguyenbui210@hcmut.edu.vn; loan.pham2304@hcmut.edu.vn; nthuy.sdh241@hcmut.edu.vn; linh.dinhdieu0712@hcmut.edu.vn; hieu.pham24062003@hcmut.edu.vn; dat.nguyenhuu@hcmut.edu.vn; tung.tran.129k19@hcmut.edu.vn; nbaduy.sdh241@hcmut.edu.vn; pqphu@hcmut.edu.vn*

[b]*Department of Metallurgy and Alloy Materials, Faculty of Materials Technology, Ho Chi Minh City University of Technology (HCMUT), 268 Ly Thuong Kiet Street, Dien Hong Ward, Ho Chi Minh City, Vietnam. E-mail: ltqanh@hcmut.edu.vn*

[c]*Vietnam National University Ho Chi Minh City (VNUHCM), Thu Duc Ward, Ho Chi Minh City, Vietnam*

† Equal contributors.

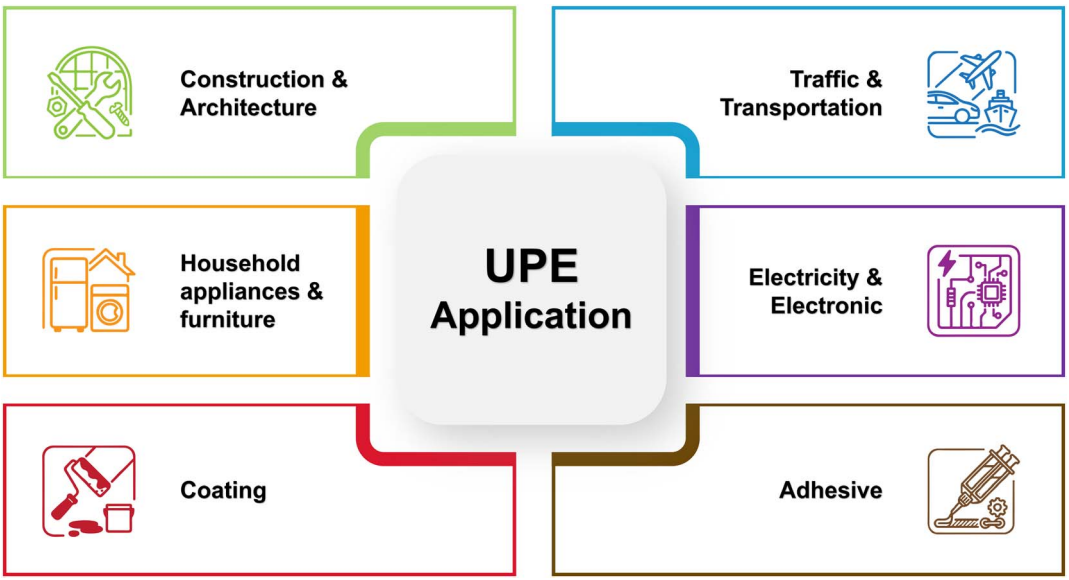


Fig. 1 Potential applications of UPE composite-based materials.

composites, making them a potential choice for UPE reinforcement.[13–17] However, a significant challenge when using carbon nanoparticles is their tendency to agglomerate due to their large surface area and high surface energy, which reduces the reinforcement efficiency, creates local defects, and prevents uniform dispersion in the polymer matrix.[14,15] To address these challenges, various approaches have been investigated to tailor and tune the properties of carbon materials, including vapor-phase hydrolysis and chemical vapor deposition (CVD). However, these methods often involve relatively complex processing routes, require high temperatures, and may employ chemicals that raise environmental concerns.[18]

To overcome this limitation, solution plasma (SP) technology has been proposed as an advanced, environmentally friendly method that does not require high-temperature conditions or toxic chemicals.[19–21] The principle of SP is based on the direct generation of plasma in the liquid phase *via* high-voltage pulses, thereby forming microplasma regions with extremely high electron temperatures, ion densities, and local pressures.[19] In these high-energy environments, free radicals and secondary electrons are continuously generated, promoting sputtering or erosion of electrodes and the formation of carbon nanoparticles.[19,21,22] High-energy particles activate styrene monomer molecules *via* electron collisions, thereby initiating direct grafting polymerization to form stable coatings or graft structures directly on the surface of newly formed nanoparticles.[23,24]

From a physicochemical perspective, the direct formation of long polymer chains on nanoparticle surfaces provides superior stabilization.[25–27] According to research by Rong *et al.*, the presence of a polymer coating significantly changes the surface energy of carbon nanoparticles.[28] This coating acts as an interfacial modifier to reduce interfacial surface tension, thereby making the liquid resin easily wettable and completely covering the nanoparticles, thereby optimizing stress transfer from the resin matrix to the filler.[29,30] Regarding the anti-aggregation mechanism, the grafted polymer chains provide steric stabilization.[25] According to a detailed analysis by Chancellor *et al.*, these polymer chains act as a strong physical barrier.[15] When nanoparticles come close together, the polymer layer creates a sufficiently large entropic repulsion to counteract the natural van der Waals attraction between the carbon particles, thereby effectively inhibiting reaggregation without the need for surfactants.[15,27] As a result, this method not only prevents agglomeration through spatial stabilization but also establishes strong chemical bonds with the UPE matrix, thereby significantly enhancing the mechanical and thermal strengthening efficiency of the composite material system.[23,24,30]

The objective of this study is to synthesize styrene-grafted carbon nanoparticles *via* liquid plasma technology and to use them as reinforcement in UPE, thereby significantly enhancing the composite's mechanical properties. The novelty of this work lies in the creation and grafting of nanocarbon surfaces onto styrene monomer in a single step using the SPP method. Unlike conventional post-modification strategies, this approach enables direct control of interfacial architecture at the nanoscale while significantly simplifying processing and reducing environmental impact. This approach not only offers opportunities to fabricate high-performance UPE-nanocarbon composite systems but also contributes to the development of sustainable green materials.[14,15,17]

## 2. Experimental

### 2.1 Materials

Unsaturated polyester (UPE) resin and the initiator methyl ethyl ketone peroxide (MEKP) were supplied by Saudi Industrial Resins (SIR, Saudi Arabia). Styrene monomer was purchased from Tan Kim Long Company (Vietnam).

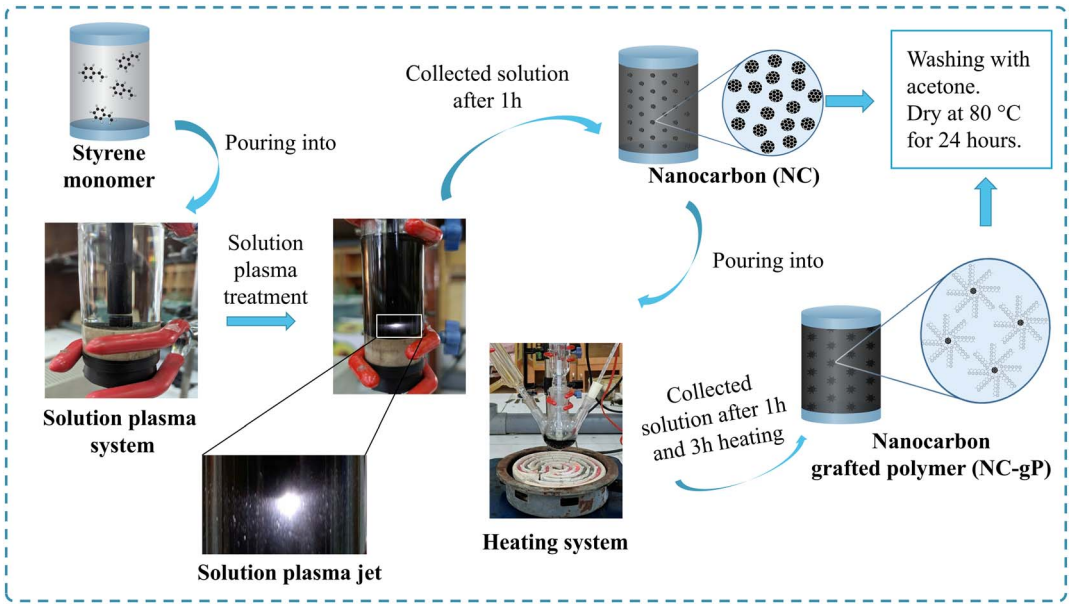


Fig. 2 Synthesis of nano carbon and styrene-grafted nano carbon particles *via* solution plasma.

## 2.2 Methods

**2.2.1 Design of the solution plasma system.** The plasma reactor was designed with electrodes positioned at approximately one-fifth of the reactor height. Two carbon electrodes, each with a diameter of 2 mm, were symmetrically mounted in the reactor through rubber stoppers. The distance between the two electrodes was 1 mm. The electrodes were insulated and connected to the plasma module's two output terminals. Plasma was initiated between the carbon electrode tips using a Vinasemi 305D DC power supply coupled with a high-voltage ignition module. The discharge was operated at 10 W with an applied voltage of 2.0 kV.

**2.2.2 Synthesis of nano carbon and styrene-grafted nano carbon particles *via* solution plasma.** A volume of 100 mL of styrene monomer (SM) was carefully introduced into a sealed reactor before the system was powered. Plasma discharge was conducted at 2.0 kV and 10 W for 1 hour to produce carbon nanoparticles (NC).[31] Subsequently, a reflux system was assembled, and the obtained NC dispersion was heated at 70 °C for 1 hour and 3 hours to promote the grafting of styrene

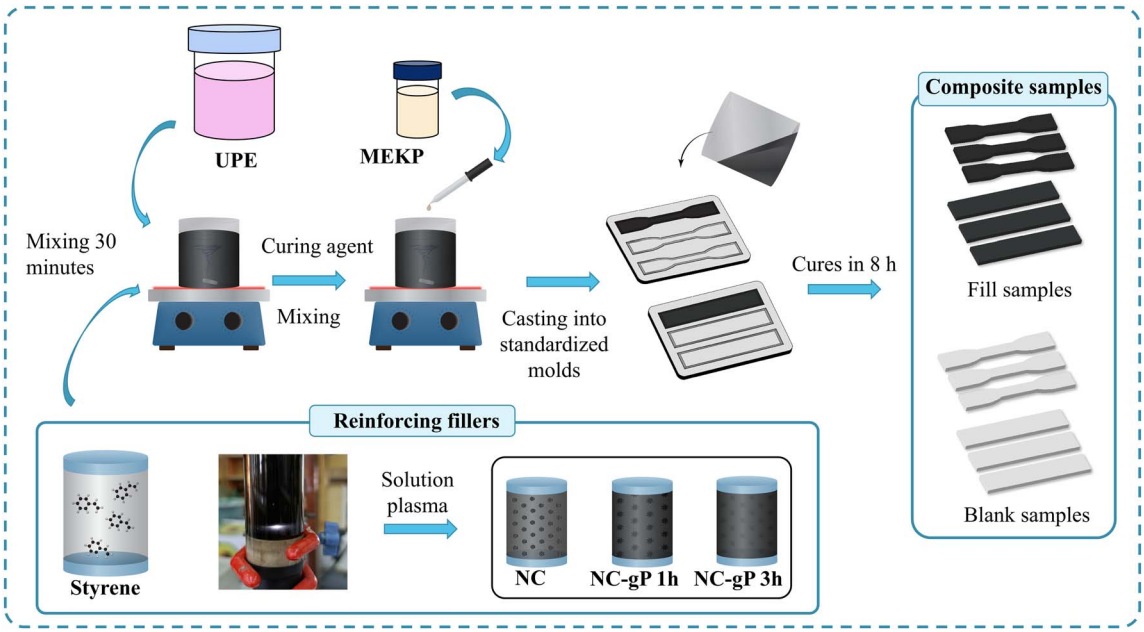


Fig. 3 Curing process of UPE resin reinforced with carbon nanoparticles.

polymer chains onto the carbon particle surface. The resulting samples were designated NC-gP(1 h) and NC-gP(3 h). To ensure that the free styrene monomer does not affect the intrinsic properties of the nanocarbon particles in the characterization analysis, a small amount of all samples, including NC, NC-gP(1 h), and NC-gP(3 h), underwent a rigorous purification process. After plasma discharge and grafting, the carbon products were separated by vacuum filtration using a 0.22 μm pore-size nylon filter.[31] The resulting carbon solids were thoroughly washed several times with acetone to remove residual styrene monomer and low-molecular-weight species, and dried in an oven at 80 °C for 24 hours.[31] The solution plasma synthesis process showed high stability and repeatability, with the average mass of recovered solid powder per batch reaching 2.47 g for NC, 2.56 g for NC-gP(1 h), and 2.87 g for NC-gP(3 h). The final purified products were stored in dark glass bottles at room temperature for analysis. A schematic diagram of the synthesis is shown in Fig. 2.

**2.2.3 Curing process of UPE resin reinforced with carbon nanoparticles.** Unsaturated polyester (UPE) resin was blended at a 4 : 1 weight ratio with SM, NC, NC-gP(1 h), and NC-gP(3 h). The resulting samples were designated as UPE/SM, UPE/NC, UPE/NC-gP(1 h), and UPE/NC-gP(3 h), respectively. Each formulation was stirred for 30 min, then the slow addition of 1 wt% MEKP was initiated to promote uniform curing. The mixtures were then stirred to ensure homogeneity, cast into silicone molds, and cured for 8 hours. The cured specimens were allowed to stabilize for 24 hours before subsequent analyses. A schematic representation of the curing process of UPE reinforced with carbon nanoparticles is shown in Fig. 3.

# 3. Characterization

## 3.1 Scanning electron microscopy (SEM)

To observe the surface morphology of the nanocarbon particles, scanning electron microscopy (SEM) was performed using a JEOL JSM-7600F instrument at the Institute of Materials Science, Vietnam. The observations were conducted at accelerating voltages of 5–10 kV, with magnifications ranging from 200× to 2000×. The samples were mounted on a metal stub with carbon tape and sputter-coated with a thin platinum (Pt) layer before analysis.

## 3.2 Fourier transform infrared spectroscopy (FTIR)

The chemical structure of the solution after plasma treatment of the styrene monomer was analyzed by Fourier-transform infrared spectroscopy (FTIR) using a Nicolet iS10 spectrometer (Thermo Scientific, Vietnam) in the wavenumber range of 4000–400 $cm^{-1}$. The spectral resolution was set at 4 $cm^{-1}$ with 32 scans.

## 3.3 Dynamic light scattering (DLS)

Dynamic light scattering (DLS) measurements were performed on a Horiba LB-550 device (Horiba Ltd., Japan) to determine the particle size of the nanocarbon. The equipment utilizes a laser diode source (650 nm, 5 mW) with a measurement range from 1 nm to 6000 nm. Samples were prepared by dispersing the nanocarbon in styrene monomer and then ultrasonicated for 30 minutes to ensure a stable, homogeneous suspension. To avoid multiple-scattering effects and ensure the signal remained within the detector's linear range, according to Horiba's recommendations, the sample concentration was kept low (approximately 0.1 mg $mL^{-1}$). Measurements were conducted at 25 °C.

## 3.4 Mechanical properties

The mechanical properties of the nanocomposites, including tensile and flexural strengths, were determined in accordance with ASTM D638 and ASTM D790, respectively. The tensile stress was calculated using eqn (1):

$$\sigma = \frac{F}{A} \tag{1}$$

where $F$ is the maximum tensile force at fracture (N), and $A$ is the cross-sectional area of the specimen ($mm^2$). For the three-point bending test, the maximum flexural stress was determined using eqn (2), in accordance with the ASTM D790 standard:

$$\sigma_f = \frac{3FL}{2bd^2} \tag{2}$$

where $F$ is the applied load at fracture (N), $L$ is the support span (mm), $b$ is the specimen width (mm), and $d$ is the specimen thickness (mm). All tests were conducted using an Instron 3369 universal testing machine (UK) at a crosshead speed of 5 mm $min^{-1}$ under ambient conditions. Each sample was tested at least five times in accordance with ASTM recommendations for the mechanical properties of composite materials, and results were reported as mean ± standard deviation (SD). The coefficient of variation (CV), defined as the ratio of the standard deviation to the mean, was calculated for each material formulation.[32–34]

# 4. Results and discussion

## 4.1 Scanning electron microscopy (SEM)

Fig. 4 presents SEM images of nanocarbon particles in different states: (a) NC, (b) nanocarbon grafted with styrene polymer for 1 hour (NC-gP(1 h)), and (c) nanocarbon grafted with styrene polymer for 3 hours (NC-gP(3 h)), observed at various magnifications. The NC sample (Fig. 4a) shows irregularly shaped particles with nanoscale features and relatively rough surfaces that tend to form small agglomerates. At higher magnification (50 nm scale), particle boundaries can still be discerned, which is characteristic of unmodified nanocarbon materials. For the NC-gP(1 h) sample (Fig. 4b), the overall particle morphology appears largely similar to that of pristine NC. The particle boundaries remain distinguishable, while the particle surfaces become relatively smoother. This observation suggests that styrene polymer chains are grafted onto the nanocarbon surface; however, the resulting polymer layer is likely too thin to completely obscure the original particle structure. Consequently, the NC-gP(1 h) sample largely retains the characteristic

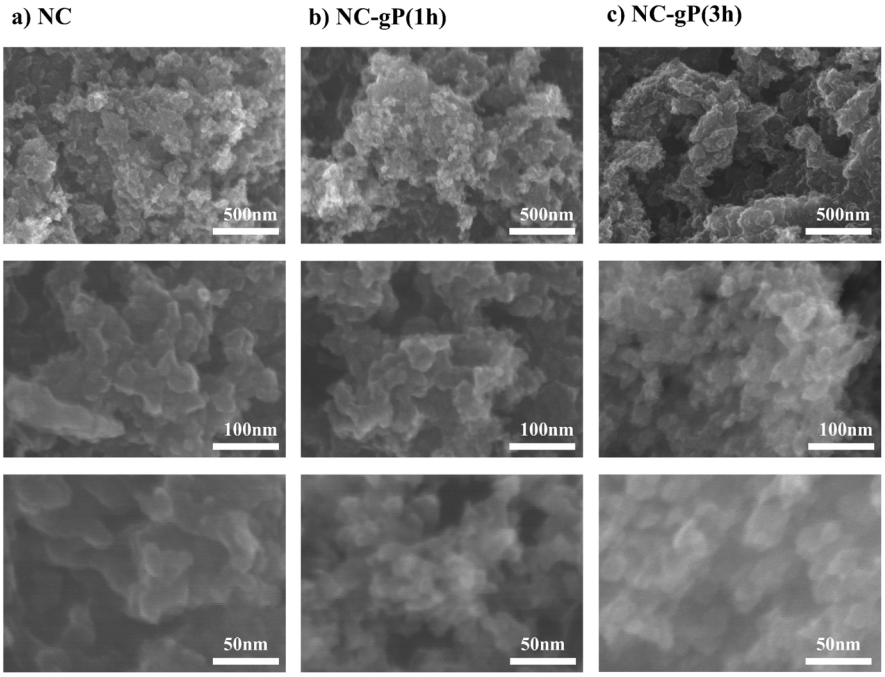


Fig. 4 SEM images illustrating the morphology of nanocarbon particles: (a) NC; (b) NC-gP(1 h); and (c) NC-gP(3 h).

morphology of nanocarbon, indicating a moderate extent of polymer grafting at this stage. Such behavior is consistent with previous reports on polymer-grafted nanoparticles, in which thin polymer coatings formed at shorter grafting times do not significantly alter the visibility of nanoscale particle boundaries, preserving optimal dispersion stability.[35] In contrast, the NC-gP(3 h) sample (Fig. 4c) exhibits a more pronounced morphological change. Individual nanocarbon particles are no longer clearly resolved; instead, larger agglomerated domains with relatively homogeneous surfaces are observed. At the 50 nm observation scale, particle boundaries are largely obscured, suggesting the formation of a relatively thick polymer layer that encapsulates the nanocarbon particles. This behavior may be attributed to prolonged grafting time, which likely promotes polymerization and polymer accumulation on the particle surface. This suggests that the 3 hours plasma treatment

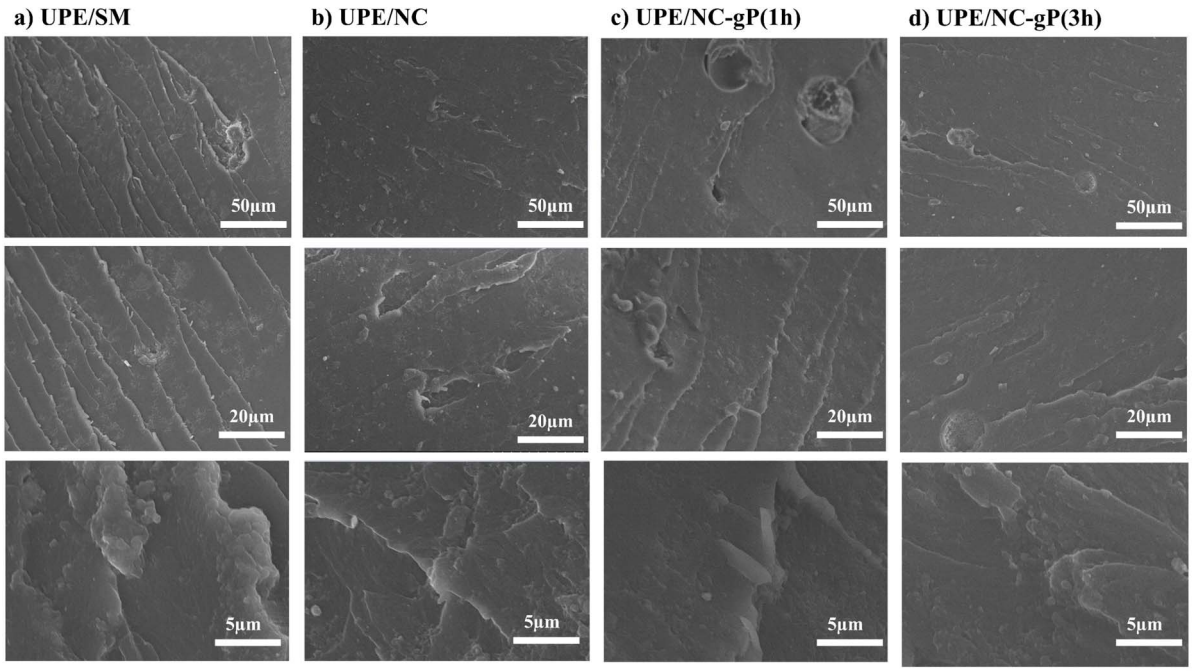


Fig. 5 SEM images illustrating the morphology of nanocomposite samples: (a) UPE/SM, (b) UPE/NC, (c) UPE/NC-gP(1 h), (d) UPE/NC-gP(3 h).

introduced a higher degree of surface functionalization, leading to increased particle coalescence. As a result, the original nanocarbon morphology becomes difficult to distinguish. This trend is consistent with RSC reports describing correlations among polymerization conditions, polymer chain length, and coating thickness on nanoparticle surfaces.[35,36]

The SEM images of the nanocomposite samples (Fig. 5) reveal pronounced differences in surface morphology and filler dispersion among the investigated materials. For the UPE/SM sample (Fig. 5a), the surface appears relatively smooth, with a low defect density. This smooth morphology can be attributed to the complete miscibility of the styrene monomer with the UPE matrix, which enables uniform blending. In the case of UPE/NC (Fig. 5b), the surface morphology becomes rougher, with numerous small, dispersed clusters visible. Compared with UPE/SM, this sample exhibits improved dispersion; however, agglomeration phenomena remain evident. This clustering is the primary factor limiting the reinforcing efficiency of the filler, a result consistent with findings reported by Pączkowski *et al.*[37] For the UPE/NC-gP(1 h) sample (Fig. 5c), the surface appears more uniform, with finely dispersed filler particles that exhibit strong interfacial adhesion to the polymer matrix. The number of observable defects is reduced, indicating a significant improvement in interfacial bonding. This result is consistent with previous studies conducted by Gulotty *et al.* and Pandey *et al.*[38,39] In contrast, the UPE/NC-gP(3 h) sample (Fig. 5d) shows the formation of larger agglomerated clusters together with a higher density of macroscopic voids. This behavior is attributed to the prolonged thermal and mechanical exposure during processing, which can weaken the structural integrity of the nanocarbon and reduce the stability of the plasma-generated surface radicals.[40] As these radicals recombine, the nanocarbon particles tend to associate into larger aggregates that are not evenly covered by the UPE matrix. In addition, localized heating accumulated during extended processing may accelerate gelation and promote partial styrene evaporation, resulting in an inhomogeneous curing network and the formation of voids. The coexistence of pronounced agglomeration and enlarged voids compromises the structural continuity of the composite, generates stress-concentration sites, and ultimately diminishes its mechanical properties. It should be noted that void formation may arise from two distinct mechanisms. On one hand, localized heat accumulation during extended processing can accelerate gelation and promote partial styrene evaporation, leading to an inhomogeneous curing network and internal microvoids.[41–43] On the other hand, surface voids observed on fractured specimens may also be generated during fracture due to interfacial debonding between the UPE matrix and NC-based phases, especially when interfacial adhesion is not sufficiently developed.[44,45]

### 4.2 Fourier transform infrared spectroscopy (FTIR)

Fig. 6 presents the FTIR spectra of pristine NC, NC-gP(1 h), and NC-gP(3 h). The pristine NC exhibits a weak and broad O–H stretching band at approximately 3300–3500 $cm^{-1}$, corresponding to surface hydroxyl groups generated during the solution plasma process, along with characteristic C=C skeletal vibrations of carbon materials in the range of 1580–1620 $cm^{-1}$.[46,47] After styrene grafting, the NC-gP samples show noticeable intensity enhancements in the C–H stretching region (~2850–3050 $cm^{-1}$) and in the aromatic C=C ring stretching region (~1450–1600 $cm^{-1}$), together with more pronounced C–H bending and ring deformation bands below 1000 $cm^{-1}$, confirming the successful attachment of styrene-derived polymer chains onto the nanocarbon surface.[31,46] No new absorption bands or significant peak shifts are observed, indicating that the grafting process mainly modifies the surface chemistry without altering the intrinsic carbon framework.[46] Notably, the NC-gP(3 h) sample exhibits stronger aromatic-related absorption and sharper C–H bending features compared to NC-gP(1 h), suggesting a higher grafting density at prolonged reaction time. This progressive surface functionalization is consistent with the enhanced interfacial adhesion observed in the UPE/NC-gP composites and correlates well with the void formation and fracture.

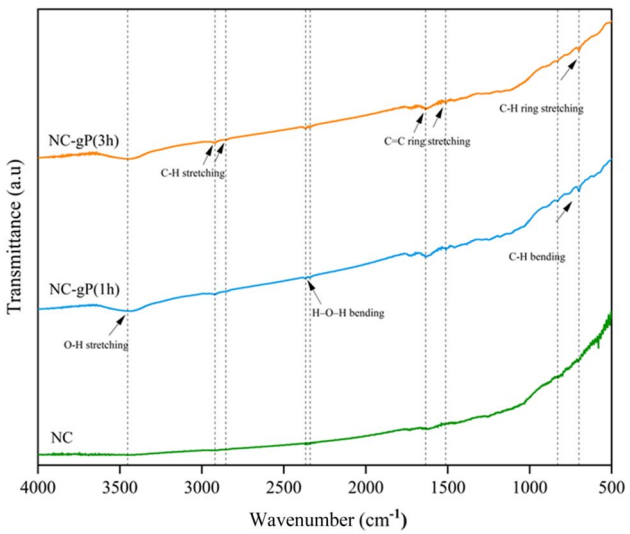


Fig. 6 FTIR spectra of NC, NC-gP(1 h), and NC-gP(3 h).

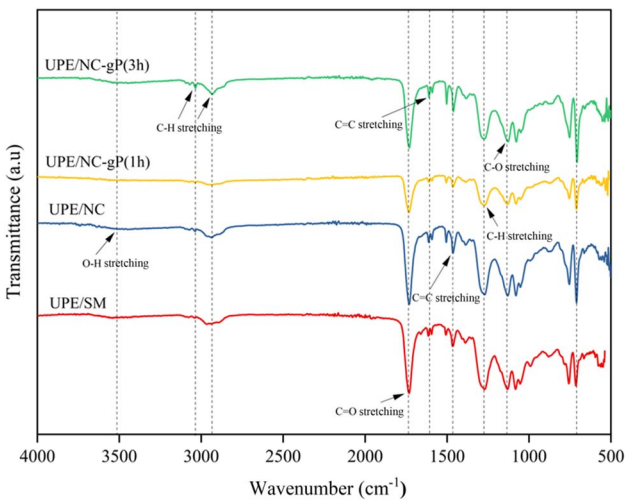


Fig. 7 FTIR spectra of nanocomposite samples.

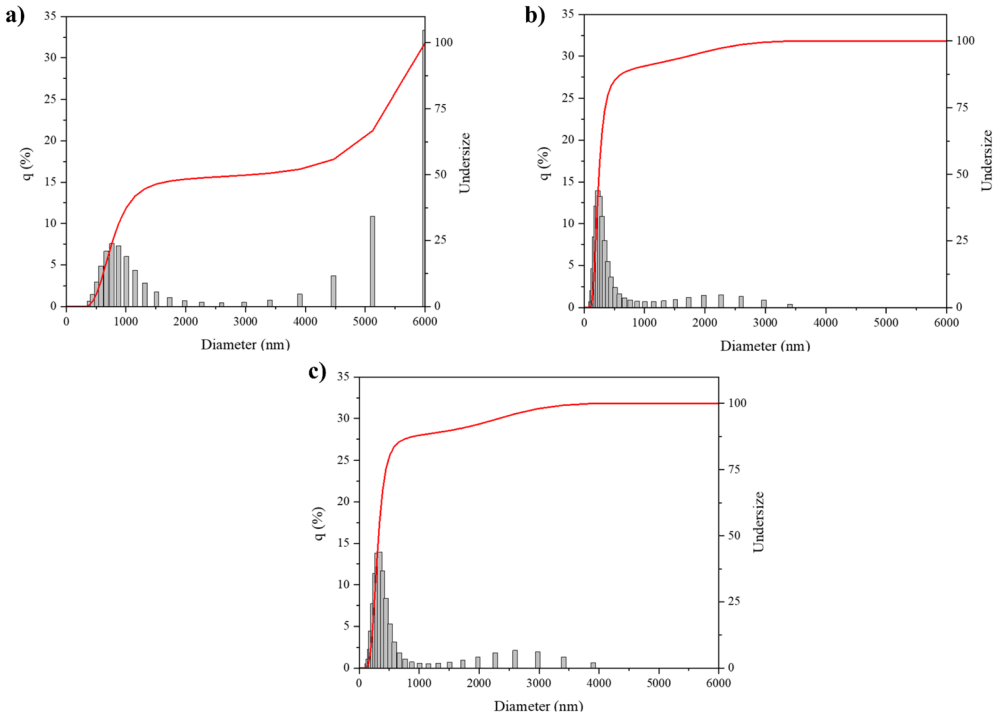


Fig. 8 Hydrodynamic size distributions of NC (a), NC-gP(1 h) (b), and NC-gP(3 h) (c) measured by DLS.

The FTIR spectra (Fig. 7) show distinct differences in the characteristic vibrational modes of functional groups across the nanocomposite samples. In the UPE/SM sample, characteristic absorption bands corresponding to C=O stretching (~1720 $cm^{-1}$), C–O stretching (~1150 $cm^{-1}$), and C–H stretching (~2900 $cm^{-1}$) typical of the UPE chemical structure, are observed.[48,49] However, no significant changes in peak intensity or position are detected, indicating limited interaction between SM and the UPE matrix. In the UPE/NC sample, in addition to the aforementioned peaks, an O–H stretching vibration (~3400 $cm^{-1}$) and a slight shift in the C=C region (~1635 $cm^{-1}$) are observed. This suggests that the plasma-solution treatment introduced new hydroxyl groups on the filler surface, potentially enhancing hydrogen bonding with the polymer matrix.[50] For the UPE/NC-gP(1 h) sample, a stronger O–H stretching band (~3430 $cm^{-1}$) appears alongside a clearly defined C=O stretching vibration (~1720 $cm^{-1}$), consistent with the increased surface functional groups observed after carbon nanofiller functionalization and their FTIR signatures.[50,51] The increased O–H peak intensity indicates activation of the nanocarbon surface, generating more reactive sites that can interact with the polymer matrix.[49] Nevertheless, the broadening of the vibrational bands suggests a non-uniform degree of interfacial bonding. Notably, the UPE/NC-gP(3 h) sample exhibits a well-resolved FTIR spectrum with distinct, minimally overlapping C–H, C=C, C=O, and C–O vibrational peaks. This suggests that the 3 hours plasma treatment introduced a higher degree of surface functionalization, thereby modifying the evolution of interphase stiffness and affecting filler–matrix interactions. These findings are consistent with previous studies reporting that hydroxyl and carbonyl groups on nanocarbon surfaces enhance adhesion to polymer matrices.[50,51]

### 4.3 Dynamic light scattering (DLS)

Fig. 8 presents the particle size distributions of pristine NC, NC-gP(1 h), and NC-gP(3 h) determined by dynamic light scattering (DLS). For the pristine NC sample (Fig. 8a), the DLS profile shows a broad size distribution, with a significant population of micrometer-sized particle aggregates. This observation suggests a strong tendency toward aggregation of unmodified nanocarbon, likely due to its high surface energy and van der Waals interactions among particles in the dispersion medium. For the NC-gP(1 h) sample (Fig. 8b), the size distribution shifts markedly toward smaller sizes and becomes narrower compared to that of pristine NC. This result suggests that styrene polymer grafting may reduce the surface energy of nanocarbon and introduce steric hindrance, thereby limiting interparticle interactions and improving the dispersion stability of the system. Such behavior is consistent with previous studies reporting that thin polymer layers formed in the early stages of grafting can effectively stabilize nanoparticles while preserving core morphology, owing to their limited thickness.[35] In contrast, the NC-gP(3 h) sample (Fig. 8c) tends toward a broader size distribution extending back to larger sizes, with the reappearance of particle aggregates in the micrometer range. The increase in hydrodynamic size may be related to the formation of a thicker grafted polymer layer at prolonged grafting times, which enhances steric entanglement and secondary aggregation between polymer chains on neighboring particles. According to reports on polymer-grafted nanoparticles, the polymer coating thickness (brush thickness) generally increases

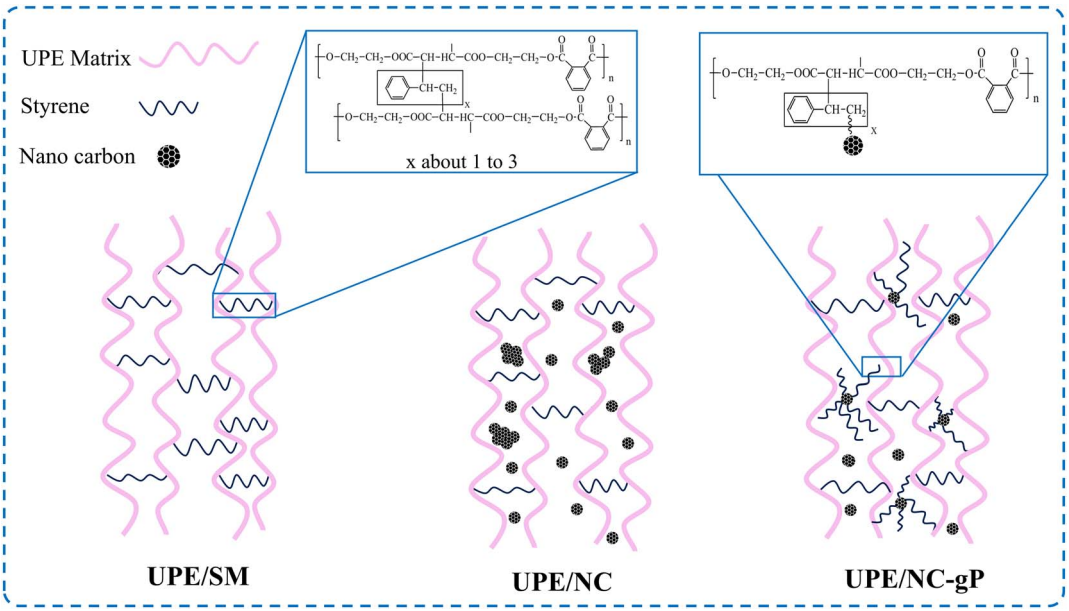


Fig. 9 The bonding mechanism of UPE and NC-gP affects the mechanical properties of nanocomposite samples.

with grafting length and density, thereby altering surface interactions and, in some cases, promoting secondary aggregation or polymer-bridging effects between particles.[36]

### 4.4 Mechanical properties

Fig. 9 shows that the mechanical properties of the samples depend on the degree of interaction among the UPE matrix, styrene, and nanocarbon. In the UPE/SM sample, styrene copolymerizes with the double bonds of UPE, forming a dense polymer network that increases stiffness but reduces ductility. When nanocarbon is incorporated (UPE/NC), the π–π and van der Waals interactions between nanocarbon and the polymer chains enhance stress transfer; however, the improvement is limited due to localized agglomeration. In the UPE/NC-gP

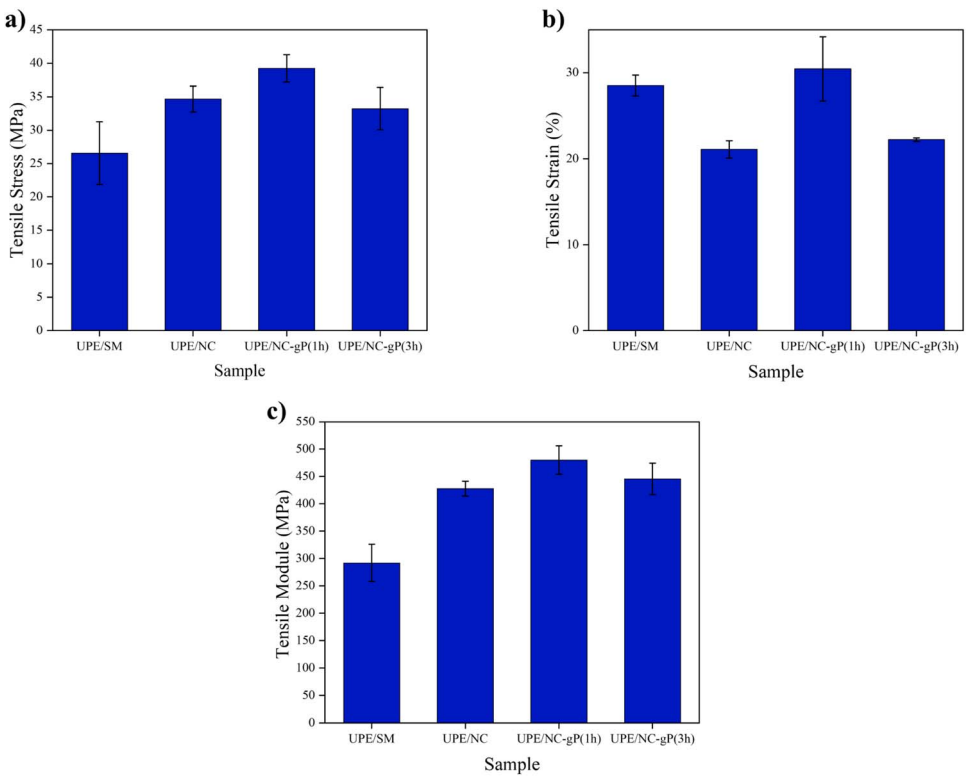


Fig. 10 Tensile stress (a), tensile strain (b) and tensile modulus (c) of the fabricated samples after tensile testing.

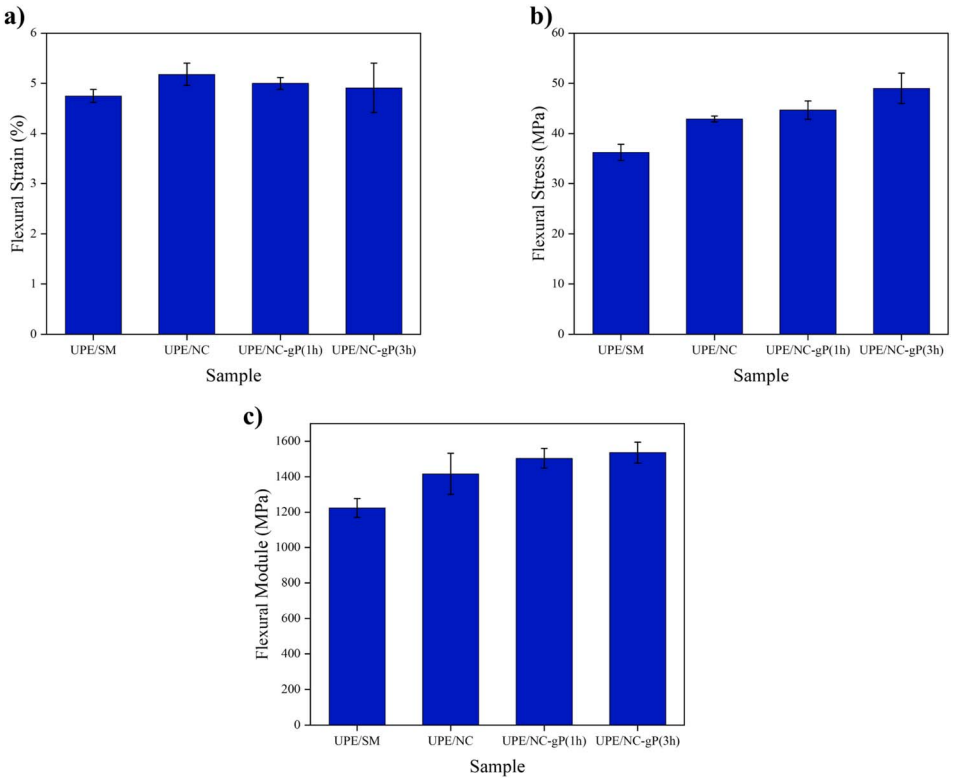


Fig. 11 Flexural stress (a), flexural strain (b), flexural modulus (c) of the fabricated samples obtained from the three-point bending test.

sample, the styrene polymer layer grafted onto the nanocarbon surface forms stable chemical bridges, improving interfacial compatibility and promoting a more uniform dispersion. Consequently, this sample achieves an optimal balance between strength, stiffness, and ductility, resulting in the highest reinforcement efficiency.[25]

**4.4.1 Tensile properties.** The results in Fig. 10 indicate that the addition of nanocarbon significantly enhanced the material's mechanical properties relative to the neat UPE/SM sample. The tensile strength of UPE/SM was only 26.56 ± 4.69 MPa, whereas that of UPE/NC increased markedly to 34.66 ± 1.93 MPa, demonstrating that nanocarbon acts as an effective reinforcing agent for the unsaturated polyester matrix.[30] Notably, the UPE/NC-gP(1 h) sample exhibited the highest tensile strength of 39.23 ± 2.06 MPa, indicating that a short grafting duration effectively improved stress transfer between the matrix and the reinforcing phase by forming an optimal, sterically stabilizing, flexible polymer coating. In contrast, when the grafting time was prolonged to 3 hours, the tensile strength of UPE/NC-gP(3 h) decreased to 33.23 ± 3.18 MPa, attributable to the formation of an excessively thick polymer layer, which led to defect-sensitive macroscopic voids that weakened interlayer interactions and initiated premature fracture.[52,53]

Similarly, this trend was also observed in the elongation at break and elastic modulus. The UPE/SM sample exhibited the highest elongation at break (28.52 ± 1.20%) due to the inherent ductility of the polymer matrix.[29,52] Upon the addition of nanocarbon, the elongation decreased to 21.09 ± 1.02% because the composite structure became stiffer and less deformable.[30] However, the presence of a thin polymer coating in the UPE/NC-gP(1 h) sample facilitated a more uniform dispersion of nanocarbon. It reduced local stress concentration, leading to a recovery in elongation at break to 30.45 ± 3.73%.[53] In contrast, an excessively thick coating layer in the UPE/NC-gP(3 h) sample restricted the matrix's plastic deformation capability, resulting in a decrease in elongation to 22.23 ± 0.21%.[29,53]

Regarding the elastic modulus, the value gradually increased from 291.96 ± 33.55 MPa (UPE/SM) to 427.69 ± 13.66 MPa (UPE/NC). It reached a maximum of 479.89 ± 26.22 MPa for the UPE/NC-gP(1 h) sample, reflecting the formation of a matrix and the reinforcing phase.[29] When the grafting time was extended to 3 hours, the modulus slightly decreased to 445.46 ± 28.96 MPa indicating that a thicker polymer coating reduced the efficiency of stress transfer across the interface.[53]

**4.4.2 Flexural properties.** Based on the flexural test results shown in Fig. 11, it can be observed that the surface modification of nanocarbon *via* styrene grafting had a pronounced effect on the flexural behavior of the UPE-based composite. Compared to the UPE/SM sample, both the flexural strength and flexural modulus of the UPE/NC composite increased significantly from 36.23 ± 1.63 to 42.92 ± 0.57 MPa, and from 1223.71 ± 53.7 to 1416.28 ± 115.57 MPa, respectively, demonstrating the reinforcing role of nanocarbon in enhancing the load-bearing capacity and stiffness of the composite.[29,30]

Notably, when styrene grafting was carried out for 1 hour, the UPE/NC-gP(1 h) sample exhibited a flexural strength of 44.67 ± 1.82 MPa and a flexural modulus of 1504.06 ± 55.18 MPa, which were higher than those of UPE/NC. This indicates that the

Table 1 Comparison of the mechanical properties of UPE/NC-gP(1 h) composites with those reported in previous studies

| Type of filler | Optimal filler content (wt%) | Tensile strength (MPa) | Young's modulus (MPa) | Flexural strength (MPa) | Flexural modulus (MPa) | Reference |
|---|---|---|---|---|---|---|
| Nanocarbon graft polymer styrene solution | 20 | 39.23 | 479.89 | 44.67 | 1504.06 | This study |
| $TiO_2$ powder | 3 | 24.76 | — | 46.67 | — | 54 |
| Coffee husks powder (CH2, 0.315–0.630 mm) | 50 | 8.60 | 1899.00 | 18.70 | 1888.50 | 55 |
| White cement (WC) | 40 | 20.81 | 850 | 43.49 | 3900.00 | 56 |
| ZnO + HFC treated jute fiber | 40 g $L^{-1}$ HFC + ZnO | 23.00 | — | 55.00 | — | 57 |
| $ZrO_2$ nanoparticles | 2.5 | — | — | 99.00 | 3800.00 | 60 |
| Oil palm shell (OPS) | 3 | 37.56 | 1150 | 75.27 | 6170.00 | 62 |
| Bamboo nanoparticles (woven) | 3 | 55.68 | 1930.00 | 75.60 | 4650.00 | 63 |

moderately formed polymer coating effectively enhanced stress transfer between the matrix and the reinforcement phase by improving interfacial compatibility and reducing local stress concentration.[53] However, when the grafting duration was extended to 3 hours, both flexural strength and modulus increased slightly ($49.01 \pm 3.03$; $1535.81 \pm 58.47$ MPa), while the flexural strain decreased to $4.91 \pm 0.49\%$, suggesting that the composite became stiffer but more brittle. A thick polymer layer surrounding the carbon nanoparticles forms a highly entangled interfacial network that effectively enhances interfacial stiffness and bending load-bearing capacity despite the internal voids of the composite material. This phenomenon can be explained by the mechanism described by Soeta *et al.* (2017).[53] The thickness of the interface layer determines the strengthening effect; an excessively thick polymer coating will alter the stress distribution by restricting chain mobility, increasing macroscopic stiffness, but limiting the plastic deformation capacity of the matrix.

In contrast, the flexural elongation exhibited an opposite trend to that of stiffness. The UPE/SM sample showed a value of $4.75 \pm 0.13\%$, which slightly increased in the UPE/NC sample ($5.18 \pm 0.22\%$) due to the good dispersion effect of nanocarbon, and remained nearly unchanged for the 1 hour grafted sample ($5.00 \pm 0.12\%$). However, when the grafting time was extended to 3 hours, the elongation decreased to $4.91 \pm 0.49\%$, indicating that a thicker polymer coating tended to restrict the plastic deformation of the resin matrix.[52]

By combining the results from both tensile and flexural tests, it can be concluded that the UPE/NC-gP(1 h) sample exhibits an optimal balance between strength, stiffness, and ductility. A 1 hour grafting time is considered the most suitable condition, allowing the formation of a moderately thick polymer layer that enhances interfacial interactions without causing particle aggregation or reducing stress-transfer efficiency, thereby providing the highest reinforcement effect for the UPE/NC composite system.

As shown in Table 1, the UPE/NC-gP(1 h) sample exhibited a tensile strength of 39.23 MPa and a flexural strength of 44.67 MPa, which are higher than those of composites containing $TiO_2$ (24.76 MPa),[54] coffee husk powder (8.6 MPa),[55] white cement (20.81–31.75 MPa),[56] ZnO combined with HFC-treated jute fiber (23 and 55 MPa),[57] fly ash (23.8 MPa),[58] and aluminum powder (12.45 MPa).[59] Compared with composites reinforced with $ZrO_2$,[60] and PET/HDPE hybrid systems,[61] although their flexural strengths are higher (99 and 55 MPa, respectively), their tensile strengths were either not improved or not reported. This comparison indicates that the present system provides a more balanced enhancement of both tensile and flexural properties, rather than improving a single mechanical parameter. The superior performance of the UPE/NC-gP(1 h) sample mainly stems from enhanced interfacial interactions induced by the styrene polymer layer grafted onto the nanocarbon surface, which improve stress transfer, promote uniform particle dispersion, and reduce agglomeration, as discussed above. Unlike conventional inorganic or natural fillers that rely primarily on mechanical or hydrogen bonding, the polymer layer grafted in this study serves as an elastic interfacial bridge between the matrix and the reinforcing phase, balancing stiffness and ductility while maintaining the composite's mechanical stability. Although the mechanical properties of the UPE/NC-gP(1 h) sample do not surpass those of the composites reinforced with OPS (37.56, 75.27 MPa),[62] and bamboo nanoparticles (55.68, 75.6 MPa),[63] these fillers possess abundant surface hydroxyl groups that facilitate strong hydrogen bonding and chemical interactions with the UPE matrix. Moreover, their high modulus and good dispersion contribute to efficient stress transfer and crack-resistance.

Overall, the UPE/NC-gP(1 h) composite exhibits superior reinforcement efficiency relative to most prior studies, confirming the effectiveness and feasibility of the solution plasma method for functionalizing the carbon material surface. This technique offers advantages for controlling reactions in liquid-phase environments, enabling the fabrication of composites with enhanced mechanical performance and structural stability, and highlighting its potential for developing high-performance polymer nanocomposite systems.

## 5. Potential applications of the material

Nanocarbon-grafted styrene (NC-gP) represents a promising direction in the design of functional polymer composite

systems, where the reinforcement efficiency and performance depend strongly on the interfacial structure and dispersion state of the carbon phase. Studies on nanocarbon-grafted polystyrene have shown that the grafted polymer layer improves dispersion, forms a continuous conductive network, and enhances interfacial interactions, thereby increasing stress-transfer efficiency in composites.[64,65] The nanocarbon in this study was fabricated using an environmentally friendly solution plasma method, yielding an activated surface that is favorable for grafting polystyrene and for interacting with the UPE matrix, thereby significantly improving compatibility and mechanical reinforcement efficiency and enabling diverse applications.

The most direct and vital application of NC-gP is as an advanced reinforcing agent for composite material systems. The polystyrene shell acts as a bridge for interfacial interactions, enhancing phase interactions and improving stress-transfer efficiency between nanocarbon and the polymer matrix, making it particularly suitable for composite materials requiring high mechanical strength and long-term stability.[64,65] Furthermore, achieving uniform dispersion of the conductive phase helps reduce the percolation threshold, thereby expanding the range of applications to antistatic and thermal management systems.[66]

In energy storage, the grafted layer provides steric stabilization, limiting re-aggregation of nanocarbon and supporting the formation of a stable three-dimensional conductive network in the electrode. This mechanism is critical for maintaining the mechanical integrity of the electrode during repeated charge–discharge cycles, a key requirement for high-performance lithium-ion batteries and supercapacitors.[31,40] Therefore, NC-gP is considered a potential candidate for polymer-carbon electrodes, where simultaneous electrical conductivity, cycle strength, and micro-deformation resistance of the carbon phase are required.

The combination of nanocarbon's electrical conductivity and polystyrene's viscoelasticity provides an ideal material platform for innovative electronic and sensor applications. The polymer shell regulates the spacing between the conductive particles, thereby enhancing tunneling and optimizing both the sensor's sensitivity and signal stability (piezoresistive).[67] Additionally, the electrochemical stability of the polystyrene-grafted nanocarbon surface opens up prospects for application in next-generation biochemical sensors with high accuracy.[68]

In the biomedical field, the polymer layer grafted onto the nanocarbon surface is considered a modifier of surface properties and dispersion state, contributing to improved material stability in complex environments. Previous studies have shown that polystyrene-based surface-modified nanocarbons can offer material-level advantages, such as hydrophobic surface shielding, thereby suggesting potential for functional delivery systems and future biodiagnostic applications.[69] This grafting process also limits fluorescence quenching from aggregation, enabling the development of fluorescence detectors with improved optical stability and sensitivity for medical imaging diagnostics.[70]

Based on analyses of structural, property, and interfacial interaction mechanisms, this study proposes potential directions for the application of NC-gP, paving the way for further research to clarify material performance in specific application contexts.

# 6. Conclusion

In this study, styrene-grafted carbon nanoparticles were successfully synthesized using the solution plasma method, a green and straightforward approach. The solution plasma process (SPP) was carried out in styrene solvent for 1 hour at 2.0 kV and 10 W. The carbon nanoparticles exhibited grafting capability, and surface-bound free radicals formed long polymer chains under reaction conditions of 70 °C for 1 hour. The tensile and flexural test results showed that the addition of nanocarbon and the adjustment of the styrene grafting time significantly affected the mechanical properties of UPE composites. Compared with the UPE/SM, the UPE/NC sample exhibited a notable increase in tensile strength (from 26.56 ± 4.69 to 34.66 ± 1.93 MPa) and tensile modulus (from 291.96 ± 33.55 to 427.69 ± 13.66 MPa), while also improving the flexural strength (from 36.23 ± 1.63 to 42.92 ± 0.57 MPa) and flexural modulus (from 1223.71 ± 53.7 to 1416.28 ± 115.57 MPa). This demonstrates that nanocarbon acts as an effective reinforcing phase. In particular, the UPE/NC-gP(1 h) sample showed the most outstanding mechanical performance, with a tensile strength of 39.23 ± 2.06 MPa, a tensile modulus of 479.89 ± 26.22 MPa, and an elongation of 30.45 ± 3.73%; it simultaneously achieved a flexural strength of 44.67 ± 1.82 MPa and a flexural modulus of 1504.06 ± 55.18 MPa. This overall improvement is attributed to the thin polymer layer formed after 1 hour of grafting, which enhances interfacial compatibility, promotes uniform dispersion of nanocarbon, and increases stress-transfer efficiency. In contrast, when the grafting time was extended to 3 hours, the polymer coating became excessively thick, triggering secondary agglomeration and defect-sensitive voids. However, the increased interfacial stiffness maintained the high flexural performance, reducing the tensile strength to 33.23 ± 3.18 MPa, the tensile elongation to 22.23 ± 0.21%, and the flexural elongation to 4.91 ± 0.49%, indicating decreased plastic deformability and reduced stress-transfer efficiency. These results show that a 1 hour grafting time yields more synergistic mechanical properties than a 3 hours grafting time, indicating a superior balance of mechanical properties. Simultaneously, the results highlight the effectiveness of the solution-plasma method in controlling the polymer grafting process, enhancing surface interactions, and improving the reinforcement efficiency of UPE materials. This finding underscores the remarkable potential of UPE nanocomposites, whose lightweight nature, good interfacial compatibility, and superior mechanical properties confer enhanced load-bearing capacity and resistance to cracking. Such characteristics make these materials highly suitable for advanced composite applications across a wide range of fields, including energy storage, electronics and sensing, biomedical and environmental technologies, and automotive, marine, construction, and other high-performance structural systems.

# Author contributions

Nguyen Bui Quynh Anh: conceptualization, methodology, investigation, validation, formal analysis, writing – original

draft; Pham Thi Phuong Loan: data curation, investigation, methodology, formal analysis, writing – original draft; Nguyen Thanh Huy: visualization, resources, methodology; Dinh Dieu Linh: investigation, validation, visualization; Pham Tri Hieu: data curation, resources, visualization; Nguyen Huu Dat: investigation, methodology, data curation; Thanh Tung Tran: investigation, validation, visualization; Luong Thi Quynh Anh: visualization, resources, methodology; Nguyen Bui Anh Duy: project administration, writing – review and editing; Phan Quoc Phu: supervision, writing – review and editing, funding acquisition. All authors gave final approval for publication and agreed to be held accountable for the work performed therein.

## Conflicts of interest

There are no conflicts to declare.

## Data availability

The data supporting the results of this study have been deposited in the Zenodo open-access repository and are available at https://doi.org/10.5281/zenodo.17582350.

## Acknowledgements

We acknowledge Ho Chi Minh City University of Technology (HCMUT), VNU-HCM for supporting this study.

## References

1 U. Haq and M. Ihsan, Applications of unsaturated polyester resins, *Russ. J. Appl. Chem.*, 2007, **80**, 1256–1269.
2 S. Thomas, M. Hosur and C. J. Chirayil, *Unsaturated Polyester Resins: Fundamentals, Design, Fabrication, and Applications*, Elsevier, 2019.
3 E. M. Ezeh, Advances in the development of polyester resin composites: a review, *World J. Eng.*, 2024, 97–117.
4 A. A. Athawale and J. A. Pandit, Unsaturated polyester resins, blends, interpenetrating polymer networks, composites, and nanocomposites: State of the art and new challenges, *Unsaturated Polyester Resins*, 2019, pp. 1–42.
5 S. Mehdipour-Ataei and E. Aram, High-end applications of unsaturated polyester composites, *Applications of Unsaturated Polyester Resins*, 2023, pp. 421–439.
6 Z. Latif, M. Ali, E.-J. Lee, Z. Zubair and K. H. Lee, Thermal and mechanical properties of nano-carbon-reinforced polymeric nanocomposites: a review, *J. Compos. Sci.*, 2023, **7**, 441.
7 H. Tabatabai, M. Janbaz and A. Nabizadeh, Mechanical and thermo-gravimetric properties of unsaturated polyester resin blended with FGD gypsum, *Constr. Build. Mater.*, 2018, **163**, 438–445.
8 S. Xue, Z. Yu, Z. Tang and Y. Liu, Simultaneous reinforcement and toughening methods and mechanisms of thermosets: a review, *Mater. Horiz.*, 2025, 10390–10413.
9 M. M. Nassar, R. Arunachalam and K. I. Alzebdeh, Machinability of natural fiber reinforced composites: a review, *Int. J. Adv. Manuf. Technol.*, 2017, **88**, 2985–3004.
10 C. Baley, A. Bourmaud and P. Davies, Eighty years of composites reinforced by flax fibres: A historical review, *Composites, Part A*, 2021, **144**, 106333.
11 T. T. L. Doan, H. M. Brodowsky, U. Gohs and E. Mäder, Re-Use of Marble Stone Powders in Producing Unsaturated Polyester Composites, *Adv. Eng. Mater.*, 2018, **20**, 1701061.
12 Z.-Y. Wang, X.-W. Cheng, J.-P. Guan, Y.-W. Zhu, X. Dong, Z. Chen, J.-J. Wang and J.-J. Xu, UV protection, antistatic and flame-retardant multifunctional coating of polyester/spandex fabric with carbon black nanoparticles, *Polym. Degrad. Stab.*, 2024, **220**, 110657.
13 J.-V. Lim, S.-T. Bee, L. T. Sin, C. T. Ratnam and Z. A. A. Hamid, A Review on the Synthesis, Properties, and Utilities of Functionalized Carbon Nanoparticles for Polymer Nanocomposites, *Polymers*, 2021, **13**, 3547.
14 N. Baig, I. Kammakakam and W. Falath, Nanomaterials: A review of synthesis methods, properties, recent progress, and challenges, *Mater. Adv.*, 2021, **2**, 1821–1871.
15 A. J. Chancellor, B. T. Seymour and B. Zhao, Characterizing polymer-grafted nanoparticles: from basic defining parameters to behavior in solvents and self-assembled structures, *Anal. Chem.*, 2019, **91**, 6391–6402.
16 S. A. Nguyen, T. Q. Dong, M. Q. Doan, N. H. Nguyen, T. A. Nguyen, X. D. Ngo, A. T. Pham and A. T. Le, Boosting the ultraviolet shielding and thermal retardancy properties of unsaturated polyester resin by employing electrochemically exfoliated e-GO nanosheets, *RSC Adv.*, 2023, **13**, 25762–25777.
17 N. Saba, M. Jawaid, H. Fouad and O. Y. Alothman, *Nanocarbon: Preparation, Properties, and Applications, Nanocarbon and its Composites*, 2019, pp. 327–354.
18 M. K. Mun, W. O. Lee, J. W. Park, D. S. Kim, G. Y. Yeom and D. W. Kim, Nanoparticles synthesis and modification using solution plasma process, *Appl. Sci. Converg. Technol.*, 2017, **26**, 164–173.
19 N. Saito, M. A. Bratescu and K. Hashimi, Solution plasma: A new reaction field for nanomaterials synthesis, *Jpn. J. Appl. Phys.*, 2017, **57**, 0102A0104.
20 L. B. Kong, W. Yan, Y. Huang, W. Que, T. Zhang and S. Li, in *Advances in Nanomaterials*, ed. M. Husain and Z. Khan, Springer, 1 edn, 2016, ch. 2, pp. 25–101.
21 C. Chokradjaroen, J. Niu, G. Panomsuwan and N. Saito, Insight on solution plasma in aqueous solution and their application in modification of chitin and chitosan, *Int. J. Mol. Sci.*, 2021, **22**, 4308.
22 D.-w. Kim, O. L. Li, P. Pootawang and N. Saito, Solution plasma synthesis process of tungsten carbide on N-doped carbon nanocomposite with enhanced catalytic ORR activity and durability, *RSC Adv.*, 2014, **4**, 16813–16819.
23 A. Swain, N. D. Anthuparambil, N. Begam, S. Chandran and J. K. Basu, Harnessing interfacial entropic effects in polymer grafted nanoparticle composites for tailoring their thermo-mechanical and separation properties, *Soft Matter*, 2025, **21**, 3443–3472.

24 X. Wu, J. Qiu, P. Liu, E. Sakai and L. Lei, Polystyrene grafted carbon black synthesis via in situ solution radical polymerization in ionic liquid, *J. Polym. Res.*, 2013, **20**, 167.
25 B. V. Basheer, J. J. George, S. Siengchin and J. Parameswaranpilla, Polymer grafted carbon nanotubes—Synthesis, properties, and applications: A review, *Nano-Struct. Nano-Objects*, 2020, **22**, 100429.
26 S. Qin, D. Qin, W. T. Ford, D. E. Resasco and J. E. Herrera, Functionalization of Single-Walled Carbon Nanotubes with Polystyrene via Grafting to and Grafting from Methods, *Macromolecules*, 2004, **37**, 752–757.
27 V. Mittal, *Surface Modification of Nanotube Fillers*, John Wiley & Sons, 2011.
28 M. Z. Rong, M. Q. Zhang and W. H. Ruan, Surface modification of nanoscale fillers for improving properties of polymer nanocomposites: a review, *Mater. Sci. Technol.*, 2006, **22**, 787–796.
29 M. K. Alam, M. T. Islam, M. F. Mina and M. A. Gafur, Structural, mechanical, thermal, and electrical properties of carbon black reinforced polyester resin composites, *J. Appl. Polym. Sci.*, 2014, **131**, 40421.
30 Z. Spitalsky, D. Tasis, K. Papagelis and C. Galiotis, Carbon nanotube–polymer composites: chemistry, processing, mechanical and electrical properties, *Prog. Polym. Sci.*, 2010, **35**, 357–401.
31 Q. P. Phan, T. C. L. Tran, T. T. Tran, T. T. H. La, X. V. Cao, T. A. Luu and T. Q. A. Luong, Synthesis of highly activated polybenzene-grafted carbon nanoparticles for supercapacitors assisted by solution plasma, *RSC Adv.*, 2024, **14**, 36610–36621.
32 A. International, *ASTM D638-14: Standard test method for tensile properties of plastics*, 2014.
33 A. International, *ASTM D790-17: Standard test methods for flexural properties of unreinforced and reinforced plastics and electrical insulating materials*, 2017.
34 Z. Shahroodi, A. Tayebi, A. M. Far, D. Zidar, K. Straka, F. Arbeiter, N. Krempl and C. Holzer, Data-driven prediction of mechanical properties in recycled fibre-reinforced polymer composites: Integrating machine learning with material–processing feature importance analysis, *J. Mater. Res. Technol.*, 2025, **41**, 687–698.
35 D. Döpping, A. Stihl, D. Voll, F. H. Schacher and P. Théato, Revisiting polymer coatings on nanoparticles: correlation between molecular weight and coating thickness in chain transfer polymerizations, *Polym. Chem.*, 2025, **16**, 2075–2082.
36 S. Pal and S. Keten, Micro-ballistic response of thin film polymer grafted nanoparticle monolayers, *Soft Matter*, 2024, **20**, 7926–7935.
37 P. Pączkowski, N. V. Sigareva, B. M. Gorelov, M. I. Terets, Y. I. Sementsov, M. T. Kartel and B. Gawdzik, The Influence of Carbon Nanotubes on the Physical and Chemical Properties of Nanocomposites Based on Unsaturated Polyester Resin, *Nanomaterials*, 2023, **13**, 2981.
38 R. Gulotty, M. Castellino, P. Jagdale, A. Tagliaferro and A. A. Balandin, Effects of functionalization on thermal properties of single-wall and multi-wall carbon nanotube-polymer nanocomposites, *ACS Nano*, 2013, **7**, 5114–5121.
39 A. K. Pandey, T. Pal, R. Sharma and K. K. Kar, Study of matrix–filler interaction through correlations between structural and viscoelastic properties of carbonous-filler/polymer-matrix composites, *J. Appl. Polym. Sci.*, 2020, **137**, 48660.
40 H. Li, G. Wang, Y. Wu, N. Jiang and K. Niu, Functionalization of carbon nanotubes in polystyrene and properties of their composites: a review, *Polymers*, 2024, **16**, 770.
41 S. B. Liu, J. F. Yang and T. L. Yu, Curing reaction of saturated aliphatic polyester modified unsaturated polyester resins, *Polym. Eng. Sci.*, 1995, **35**, 1884–1894.
42 C. May, *Epoxy Resins: Chemistry and Technology*, Routledge, 2018.
43 C. H. Park and L. Woo, Modeling void formation and unsaturated flow in liquid composite molding processes: a survey and review, *J. Reinf. Plast. Compos.*, 2011, **30**, 957–977.
44 D. Hull, *An Introduction to Composite Materials*, Cambridge University Press, 1998.
45 J. K. Kim and Y. W. Mai, *Engineered Interfaces in Fiber Reinforced Composites*, Elsevier, 1998.
46 B. Liao, W. Wang, P. Long, B. He, F. Li and Q. Liu, Synthesis of fluorescent carbon nanoparticles grafted with polystyrene and their fluorescent fibers processed by electrospinning, *RSC Adv.*, 2014, **4**, 57683–57690.
47 S. Yaqoob, Z. Ali, S. Ali and A. D'Amore, Polystyrene–carbon nanotube composites: Interaction mechanisms, preparation methods, structure, and rheological properties—A review, *Physchem*, 2025, **5**, 14.
48 S. S. Ray and M. Okamoto, Polymer/layered silicate nanocomposites: a review from preparation to processing, *Prog. Polym. Sci.*, 2003, **28**, 1539–1641.
49 N. Yavari, M. Poorabdollah and L. Rajabi, Graphene oxide and silane-modified graphene oxide/unsaturated polyester resin nanocomposites: a comparative cure kinetic and diffusion study, *Thermochim. Acta*, 2022, **707**, 179081.
50 A. K. M. M. Alam, M. D. H. Beg, R. M. Yunus, M. Bijarimi, M. F. Mina, K. H. Maria and T. Mieno, Modification of structure and properties of well-dispersed dendrimer coated multi-walled carbon nanotube reinforced polyester nanocomposites, *Polym. Test.*, 2018, **68**, 116–125.
51 O. Nabinejad, D. Sujan, M. E. Rahman, W. Y. H. Liew and I. J. Davies, Hybrid composite using natural filler and multi-walled carbon nanotubes (MWCNTs), *Appl. Compos. Mater.*, 2018, **25**, 1323–1337.
52 H. Sharma, G. Arora, M. K. Singh, S. M. Rangappa, P. Bhowmik, R. Kumar, S. Debnath and S. Siengchin, From composition to performance: Structural insights into polymer composites, *Next Mater.*, 2025, **8**, 100852.
53 H. Soeta, S. Fujisawa, T. Saito and A. Isogai, Interfacial layer thickness design for exploiting the reinforcement potential of nanocellulose in cellulose triacetate matrix, *Compos. Sci. Technol.*, 2017, **147**, 100–106.
54 R. J. Mizban and W. H. Jassim, The Effect of Nano Sized TiO2 Particles on Improving the Stress Resistance and Thermal Stability of Unsaturated Polyester, *Ibn Al-Haitham J. Pure Appl. Sci.*, 2025, **38**, 114–124.

55 N. A. T. Huynh, T. N. Ly and M. K. Dao, Composite materials based on UPE resin and coffee husks, *J. Tech. Educ. Sci.*, 2022, **17**, 121–129.
56 S. M. Al-Mufti, A. Almontasser and S. J. Rizvi, Unsaturated polyester resin filled with cementitious materials: a comprehensive study of filler loading impact on mechanical properties, microstructure, and water absorption, *ACS Omega*, 2023, **8**, 20389–20403.
57 S. U. Zaman, S. Shahid, K. Shaker, Y. Nawab, S. Ahmad, M. Umair, Z. Khaliq and F. Azam, Development and characterization of chemical and fire resistant jute/unsaturated polyester composites, *J. Text. Inst.*, 2022, **113**, 484–493.
58 S. Zahi, Enhanced properties of fly ash-reinforced unsaturated polyester composites, *Int. J. Mater. Eng. Innovat.*, 2013, **4**, 241–257.
59 K. S. Mohan, N. M. Awad, W. A. Hussein and A. J. Farhan, Influence of Aluminum Fine Powder Content on the Some Mechanical Properties of Epoxy and Polyester Composites, *IOP Conf. Ser. Mater. Sci. Eng.*, 2020, **757**, 012005.
60 S. P. B. Sousa, M. C. S. Ribeiro, P. R. O. Nóvoa, C. M. Pereira and A. J. M. Ferreira, Mechanical behaviour assessment of unsaturated polyester polymer mortars filled with nano-sized Al2O3 and ZrO2 particles, *Cienc. Tecnol. Mater.*, 2017, **29**, e167–e171.
61 S. M. Hashim and W. Bdaiwi, Multifunctional UPE Composites Reinforced with Recycled PET/HDPE Hybrids, *Rev. Compos. Matériaux Avancés*, 2025, **35**, 733.
62 E. Rosamah, M. S. Hossain, H. P. S. A. Khalil, W. O. W. Nadirah, R. Dungani, A. S. N. Amiranajwa, N. L. M. Suraya, H. M. Fizree and A. K. M. Omar, Properties enhancement using oil palm shell nanoparticles of fibers reinforced polyester hybrid composites, *Adv. Compos. Mater.*, 2017, **26**, 259–272.
63 E. Rosamah, H. P. S. Abdul Khalil, S. W. Yap, C. K. Saurabh, P. M. Tahir, R. Dungani and A. F. Owolabi, The role of bamboo nanoparticles in kenaf fiber reinforced unsaturated polyester composites, *J. Renew. Mater.*, 2018, **6**, 75–86.
64 B. Fragneaud, K. Masenelli-Varlot, A. Gonzalez-Montiel, M. Terrones and J. Y. Cavaillé, Mechanical behavior of polystyrene grafted carbon nanotubes/polystyrene nanocomposites, *Compos. Sci. Technol.*, 2008, **68**, 3265–3271.
65 D. Qian, E. C. Dickey, R. Andrews and T. Rantell, Load transfer and deformation mechanisms in carbon nanotube-polystyrene composites, *Appl. Phys. Lett.*, 2000, **76**, 2868–2870.
66 M. Zhang, C. Zhang, Z. Du, H. Li and W. Zou, Preparation of antistatic polystyrene superfine powder with polystyrene modified carbon nanotubes as antistatic agent, *Compos. Sci. Technol.*, 2017, **138**, 1–7.
67 N. Guzenko, M. Godzierz, K. Kurtyka, A. Hercog, K. Nocoń-Szmajda, A. Gawron, U. Szeluga, B. Trzebicka, R. Yang and M. H. Rümmeli, Flexible Piezoresistive Polystyrene Composite Sensors Filled with Hollow 3D Graphitic Shells, *Polymers*, 2023, **15**, 4674.
68 W. Liu, J. Xiao, C. Wang, H. Yin, H. Xie and R. Cheng, Synthesis of polystyrene-grafted-graphene hybrid and its application in electrochemical sensor of dopamine, *Mater. Lett.*, 2013, **100**, 70–73.
69 G. Gul, R. Faller and N. Ileri-Ercan, Polystyrene-modified carbon nanotubes: promising carriers in targeted drug delivery, *Biophys. J.*, 2022, **121**, 4271–4279.
70 B. Liao, P. Long, B. He, S. Yi, Q. Liu and R. Wang, Surface grafting of fluorescent carbon nanoparticles with polystyrene via atom transfer radical polymerization, *Carbon*, 2014, **73**, 155–162.